Wavelength division multiplexing splitter with directional photonic crystal waveguide couplers

CHENG-YANG LIU*
Department of Mechanical and Electro-Mechanical Engineering, Tamkang University, New Taipei City, Taiwan

In this paper, we have investigated photonic crystal based optical waveguides implemented into wavelength division multiplexing systems. The wavelength division multiplexing splitters based on a photonic crystal waveguide coupler with square lattice and triangle lattice are proposed. The wavelength multiplexing properties are numerically investigated by using the finite-difference time-domain method. The coupling length can be reduced by using triangle lattice in the photonic crystal waveguide coupler. The symmetrical splitter has two identical photonic crystal waveguide couplers and three output channels that splits a lightwave equally and transfers power to the opposite guide. The asymmetrical splitter has two different photonic crystal waveguide couplers and three output channels that output different wavelengths to the three output channels. Compared with traditional optical coupler, the sizes of PC coupler are expected to be drastically reduced from a few hundreds of micrometers to a few tens of micrometers. The PC couplers and splitters should enable novel utilizations for designing compact devices in photonic circuits.

(Received December 24, 2013; accepted September 11, 2014)

Keywords: Wavelength division multiplexing, Splitter, Photonic crystal

1. Introduction

The propagation of electromagnetic waves in periodic dielectric structures is an interesting study in the recent years [1,2]. The periodic dielectric structures exhibit the forbidden regions of frequency where incident lightwaves cannot propagate in the any direction for any polarizations. The periodicity of photonic crystal (PC) structures is broken by introducing some point or line defects that allow PC structures for guiding lightwaves in distinct wavelength ranges [3]. Since these periodic structures have the ability to control lightwave propagation, it is a good possibility to implement PC based optical waveguides. Such PC structures can be used to design efficient compact optical components. The multiplexing and demultiplexing of optical signals are a great interest for optical communication systems [4,5]. Many optical wavelength division multiplexing (WDM) systems have been discussed with point-to-point core networks [6,7]. The WDM networks require highly accurate wavelength control of the light source and the wavelength multiplexer. Along these lines, WDM networks have been proposed using various technologies such as planar lightwave circuit based array waveguide grating [8,9] and fiber gratings [10]. However, these typical devices have dimensions of the order of centimeters or meters to support a large number of sufficient spaced wavelength channels. Therefore, all kinds of multiplexing and demultiplexing with PC structures which consist of several kinds of defects as substitution defects, interstitial defects and microcavities have been realized [11]. It has been demonstrated that PC structures can be used to multiplex and demultiplex optical signals. Recently, the multiplexer and demultiplexer based on PC waveguide are presented [12-22], and it is especially appropriate for WDM systems. These PC devices can be placed directly over photonic circuits with no increase of the optical losses. The photonic devices based on PC structures have many advantages such as relatively compact sizes and convenient integration into conventional devices.

In this paper, the square lattice and triangle lattice PC waveguide couplers WDM splitters are proposed. The wavelength multiplexing properties are numerically investigated by using the finite-difference time-domain (FDTD) calculation. It has been demonstrated accurately by comparing with the time-domain beam propagation method [12] based on a finite element scheme. The novel PC waveguide coupler based on triangle lattice PCs is presented to work in the shorter wavelength region. The demonstrations of the new WDM splitters are presented. They are constructed by symmetrical and asymmetrical PC waveguide couplers and have different wavelength multiplexing properties. The symmetrical PC waveguide WDM splitters have two square or triangle lattice PC waveguide couplers at the same coupling lengths. The asymmetrical PC waveguide WDM splitters have two square or triangle lattice PC waveguide couplers at different coupling lengths. The numerical method used in this paper is presented in Section 2. The design and simulation of PC waveguide coupler are shown in Section

3. The design and simulation of PC WDM splitter are shown in Section 4. The potential applications and the conclusion for PC waveguide coupler and splitter are summarized in Section 5.

2. Numerical method

In 1966, the FDTD method is first proposed by Yee [23]. The time-dependent Maxwell's equations are separated using central-difference approximations to the time and space partial derivatives. The FDTD calculations have emerged as primary facility to compute many scientific and engineering problems for dealing with electromagnetic wave interactions in different materials and structures. In this paper, the two-dimensional (2-D) FDTD method is used to simulate the lightwave propagation in the 2-D PC waveguides. The numerical absorbing boundary conditions are applied to the computational region of the FDTD algorithm. The whole computational domain is surrounded by perfectly matched layers to absorb the outgoing lightwaves [24]. In 2-D simulations, the computational domain is in the x-z plane. We assume that the device being modeled extends to infinity in the y-direction with no change in the form or position of its transverse cross section. The PC waveguide devices are laid out in the x-z plane. Here, Δx and Δy are the lattice space increments in the x and y coordinate directions, respectively. The incident lightwave is uniform in the y-direction, then all partial derivatives of the electromagnetic fields with respect to y must equal zero. The lightwave propagation is along z-direction. The space sampling is a sub-wavelength scale and assumed $\Delta x = 0.07$ and $\Delta z = 0.07$. Each mesh point is associated with a specific material and contains the properties of materials such as dispersion parameters and refractive index. The time sampling is determined by the Courant limit to ensure the stability of the numerical algorithm. During the process of calculation, a 2-D computational region of 32 μm x 10 μm is discretized with uniform mesh. The centered finite difference expressions are used for the space and time derivatives that are both calculated and second-order accurate in the space and time increments. In order to receive the full amplitude information of lightwave, the stationary complex fields are needed. The complex fields are the source of all valuable information such as overlap integrals, reflected and output powers. These complex fields are calculated by a real-time Fourier transform performed in the last time period of the calculation. The Final complex electromagnetic fields can be visualized at particular planes located properly in the computational region. The programming of FDTD is written in MATLAB®. The computer used in the calculation is Intel® Core i7 and has 24 GB of random-access memory. The reference of FDTD method is given in [23].

3. PC waveguide coupler

In optical communication system, the conventional WDM devices provide up to 8 channels in the third transmission window (C-Band) of silica fibers around 1550 nm. The International Telecommunication Union standardized a channel spacing grid for WDM systems by using the wavelengths from 1270 nm through 1610 nm with a channel spacing of 20 nm. For the 1550 nm center wavelength, we consider the PC structure composed of a square array of dielectric cylinders in air with lattice constant a = 0.54 μm. The refractive index and the radius of cylinders are taken as n = 3.4 and r = 0.18a. Fig. 1 shows the photonic band structure for the dielectric cylinders of square array by using the plane wave expansion calculation [25], where the inset indicates the Brillouin zone of square lattice. This PC structure has a photonic bandgap for TM mode which extends from λ = 1.2 μm to 1.7 μm, where λ is the wavelength in free space. The geometrical structure of the investigated PC waveguide directional coupler is proposed. Fig. 2 shows the PC waveguide coupler with two rows of dielectric cylinders in the interaction region, where L_c is the coupling length. We can see that at some coupling length the lightwave migrates from the first waveguide to the second. The normal mode theory is employed to calculate the coupling length [26]. Total electromagnetic field $\Psi(x,z)$ in the coupling region can be represented by the superposition of excited modes:

$$\Psi(x,z) = c_1\psi_1(x,z)e^{-j\beta_1 z} + c_2\psi_2(x,z)e^{-j\beta_2 z} \quad (1)$$

where the field excitation coefficient is c_m, the localized Bloch wave function with propagation constant of β_m is $\psi_m(x,z)e^{-j\beta_m z}$, and subscript *m* marks order of mode. Total electromagnetic field $\Psi(x,L)$ should satisfy following condition after propagating coupling length z = L that a two-folded image can be made:

$$\Psi(x,L) = c_1\psi_1(x,L)e^{-j\beta_1 L} + c_2\psi_2(x,L)e^{-j\beta_2 L} = [c_1\psi_1(x,L) - c_2\psi_2(x,L)]e^{-j\beta_1 L} \quad (2)$$

The equation for coupling length can be derived by inspecting Eq. (2):

$$L = \frac{\pi}{|\beta_2 - \beta_1|} \quad (3)$$

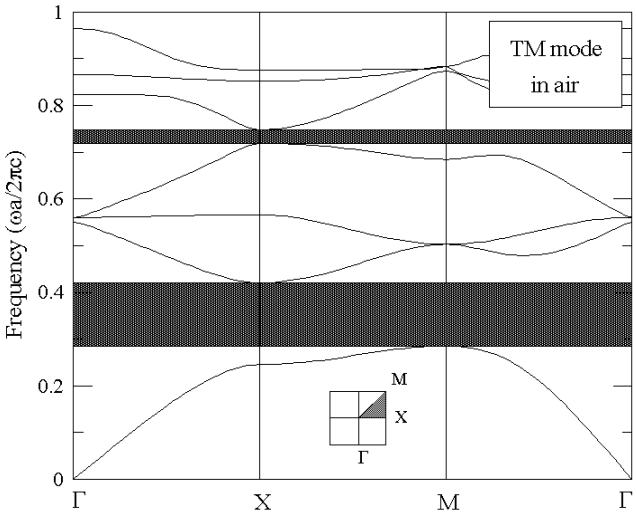

Fig. 1. Photonic band structure for the square array of dielectric columns, where inset shows the Brillouin zone.

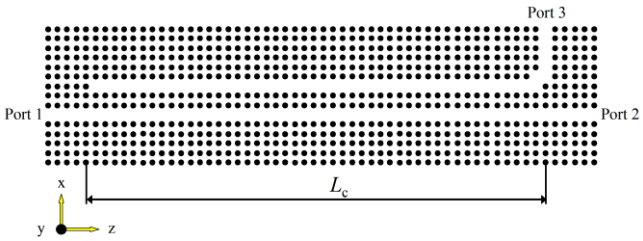

Fig. 2. PC waveguide coupler with the square lattice. The lattice constant is a = 0.54 μm and the radius of cylinders are r = 0.18a.

Fig. 3 depicts the coupling lengths of a square lattice PC waveguide coupler with two rows of cylinders in the interaction area. The different incident wavelengths need different coupling lengths for complete optical coupling. The shorter incident wavelengths need longer coupling lengths, and the longer wavelengths need shorter coupling lengths. Fig. 4 depicts the transmission spectrum for the PC waveguide coupler with $L_c = 48a$, where the incident lightwave launched into port 1 is the TM-polarized continuous wave with Gaussian profile. The unit of normalized power in the transmission spectrum is an arbitrary unit. Lightwaves with wavelengths of $\lambda_1 = 1.42\mu m$ and $\lambda_3 = 1.57\mu m$ are transferred to the opposite guide (port 3), and the lightwaves with wavelengths of $\lambda_2 = 1.52\mu m$ and $\lambda_4 = 1.62\mu m$ are outputted from the original guide (port 2). The power ratio between output ports is defined as Port 3 / Port 2 or Port 2 / Port 3. In the square lattice, the output power ratios of PC coupler are 27.51 dB at input wavelength 1.42 μm and 27.61 dB at input wavelength 1.52 μm.

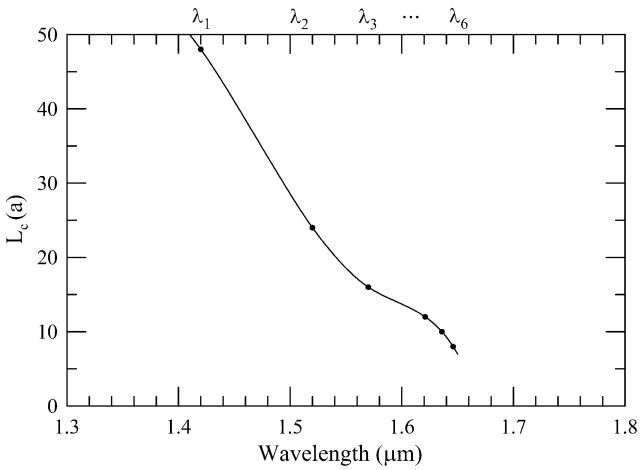

Fig. 3. Coupling lengths of the square lattice PC waveguide coupler.

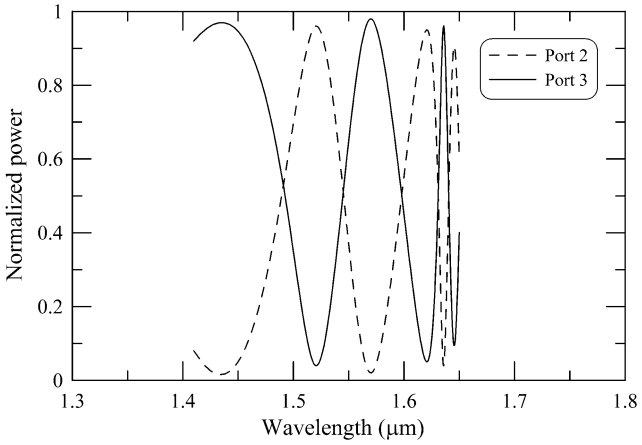

Fig. 4. Transmission spectrum of the square lattice PC waveguide coupler. The unit of normalized power is an arbitrary unit.

Fig. 5 depicts the photonic band structure of the PC with the triangle array of dielectric cylinders where the inset is the Brillouin zone of triangle lattice. We can see that the photonic bandgaps of the square and triangle PC structures are similar. The PC waveguide coupler composed of a triangle array of dielectric cylinders in air is proposed. The material properties and geometry dimensions of triangle lattice PC waveguide are the same as those of square lattice PC, as shown in Fig. 6. Fig. 7 shows the coupling lengths of the triangle lattice PC waveguide coupler. The coupling lengths also decrease as input wavelengths increase. The coupling length of 48a is satisfied by the coupling length at wavelength $\lambda_1^{'}$. At the same coupling length $L_c = 48a$, the PC waveguide coupler with triangle lattice requests shorter input

wavelength than the PC coupler with square lattice, as $\lambda_1' = 1.38\mu m < \lambda_1 = 1.42\mu m$. Fig. 8 shows the transmission spectrum for the triangle lattice PC waveguide coupler with $L_c = 48a$. The incident lightwave launched into port 1 is also the TM-polarized continuous wave with Gaussian profile. Figure 9 shows the electric field patterns at the input wavelengths $\lambda_1' = 1.38\mu m$, $\lambda_2' = 1.43\mu m$, $\lambda_3' = 1.46\mu m$, and $\lambda_4' = 1.51\mu m$. The input lightwaves with wavelengths of λ_1' and λ_3' propagate to the opposite guide (port 3), and the input lightwaves with wavelengths of λ_2' and λ_4' output from the original guide (port 2). In the triangle lattice, the output power ratios of PC coupler are 27.42 dB at input wavelength 1.38 μm and 26.95 dB at input wavelength 1.43 μm. It can be concluded that the mismatch losses have an almost negligible effect on the output power ratio. However, the output power ratio may be impaired due to different radiation losses if a three-dimensional simulation is considered. The influence of radiation losses on the performance of the PC coupler will be addressed in future work. The directional coupler is a very important device in the optical integrated circuits. To study the use of PC waveguide directional coupler, it becomes mandatory to know about the variation of the coupling length against the optical wavelength. The wavelength-dependence of the coupling length allows us to employ the PC coupler for WDM applications such as channel interleavers and wavelength demultiplexers.

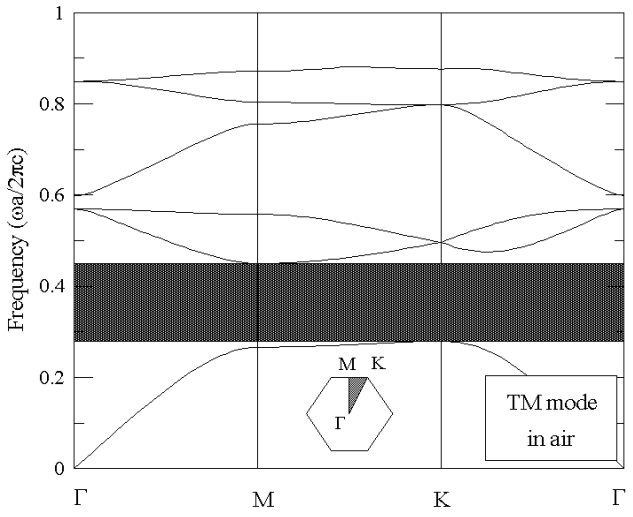

Fig. 5. Photonic band structure for the triangle array of dielectric columns, where inset shows the Brillouin zone.

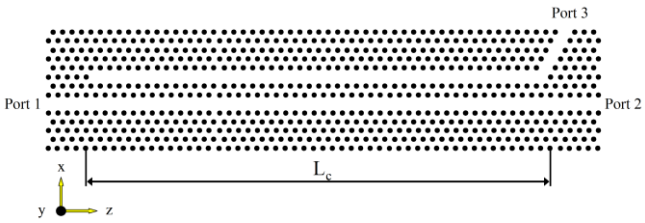

Fig. 6. PC waveguide coupler with the triangle lattice.

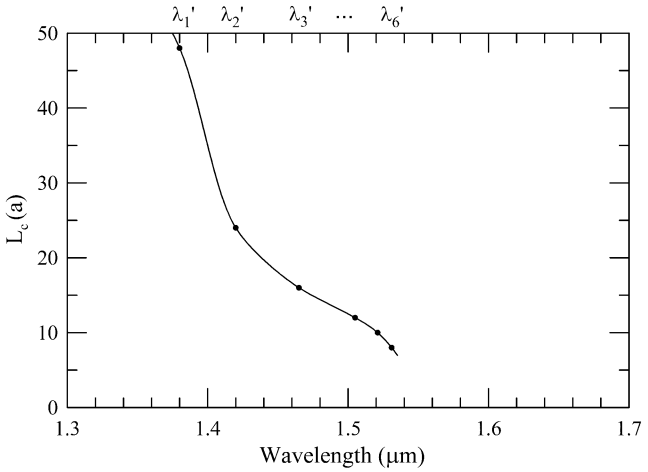

Fig. 7. Coupling lengths of the triangle lattice PC waveguide coupler.

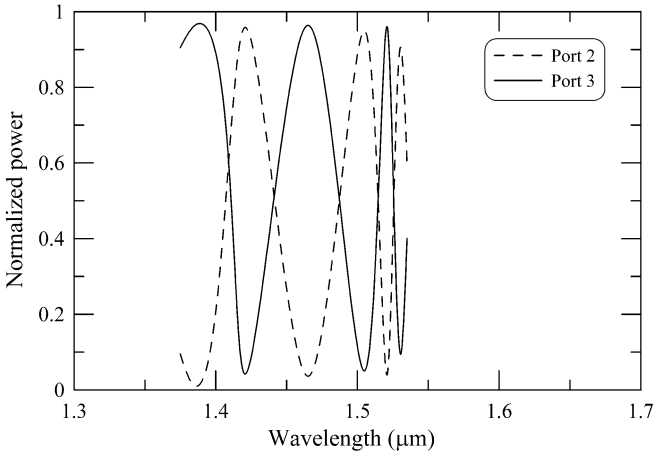

Fig. 8. Transmission spectrum of the triangle lattice PC waveguide coupler.

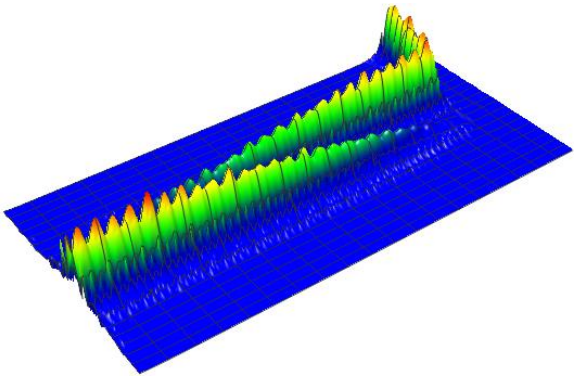

(a) Input wavelength $\lambda_1^{'}$ *= 1.38 μm*

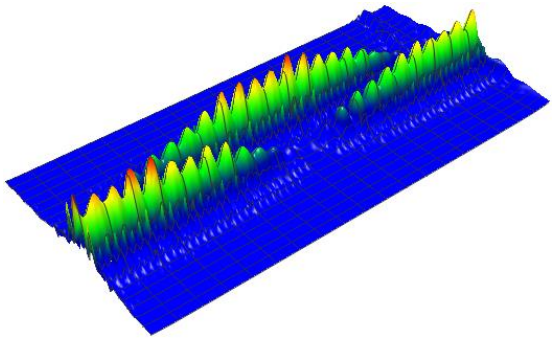

(b) Input wavelength $\lambda_2^{'}$ *= 1.43 μm*

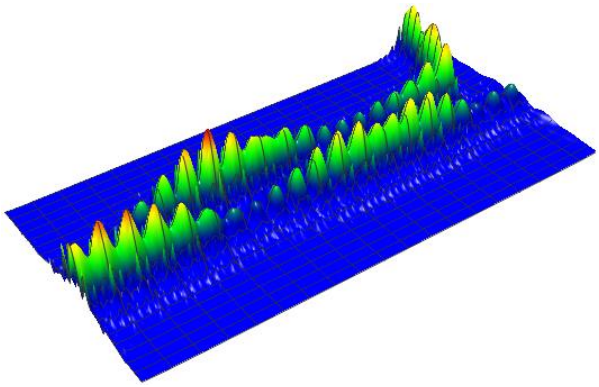

(c) Input wavelength $\lambda_3^{'}$ *= 1.46 μm*

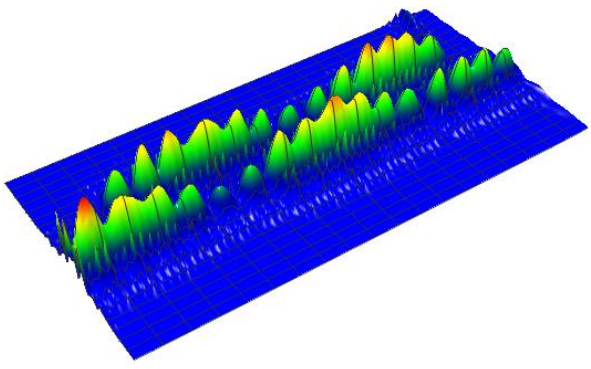

(d) Input wavelength $\lambda_4^{'}$ *= 1.51 μm*

Fig. 9. Electric field patterns of the triangle lattice PC waveguide coupler for different input wavelengths.

4. WDM splitter

The WDM splitter based on the square lattice PC waveguide couplers with three output channels is proposed and shown in Fig. 10. Fig. 11 shows the transmission spectrum for the WDM splitter at $L_c = 48a$. The WDM splitter split the power of input lightwaves equally into the opposite guide (port 3, port 4), if the wavelengths of input lightwave are odd numbers. Fig. 12 shows the electric field patterns at the input wavelengths λ_1, and λ_2. The input lightwave at wavelength λ_1 is transferred equally to the two opposite guides (port 3, port 4). The input lightwave at wavelength λ_2 is outputted from the original guide (port 2). Fig. 13 shows the multiplex signals with wavelength λ_1 and λ_2 launched into port 1 at the same time and they are outputted from ports 2-4, respectively. The wavelength multiplexing properties of the WDM splitter are numerically investigated. The WDM splitter with asymmetrical square lattice PC waveguide couplers is proposed and shown in Fig. 14. One of the waveguide couplers has coupling lengths which are half of the coupling lengths of the other waveguide coupler. Fig. 15 shows the transmission spectrum for this WDM splitter at $L_c = 48a$. The input lightwave at wavelength λ_1 is transferred to the opposite guide (port 3). The input lightwave at wavelength λ_2 is outputted from the original guide (port 2). The input lightwave at wavelength λ_3 is transferred to another opposite guide (port 4). Fig. 16 shows the electric field patterns at the input wavelengths λ_1, λ_2, and λ_3. The wavelength multiplexing properties are clearly evident.

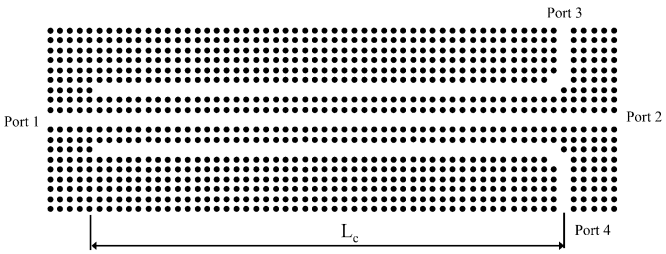

Fig. 10. PC WDM splitter with square lattice.

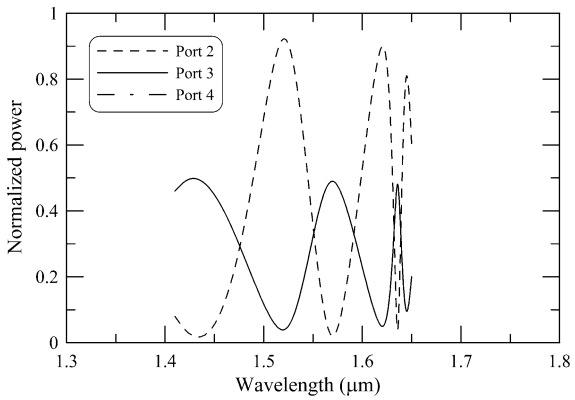

Fig. 11. Transmission spectrum of the square lattice PC WDM splitter.

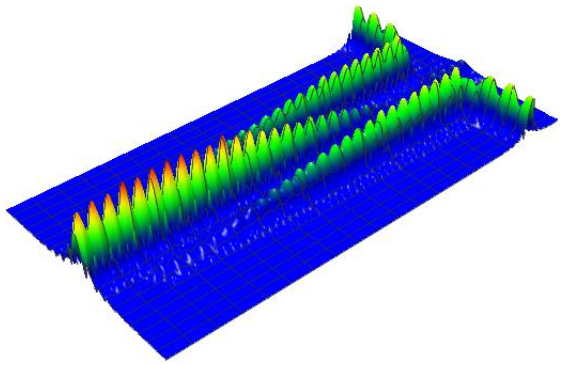

(a) Input wavelength λ_1 *= 1.42 μm*

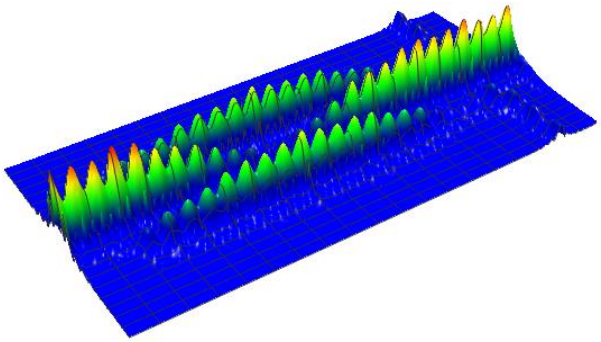

(b) Input wavelength λ_2 *= 1.52 μm*

Fig. 12. Electric field patterns of the square lattice PC WDM splitter for different input wavelengths.

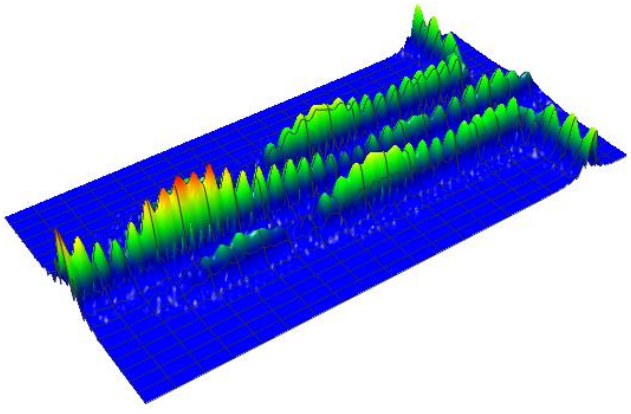

Fig. 13. Electric field patterns of the square lattice PC WDM splitter at input wavelength λ_1 *= 1.42 μm and* λ_2 *= 1.52 μm.*

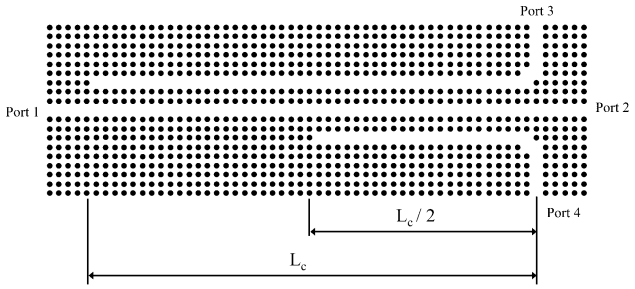

Fig. 14. Square lattice PC WDM splitter with asymmetrical PC couplers.

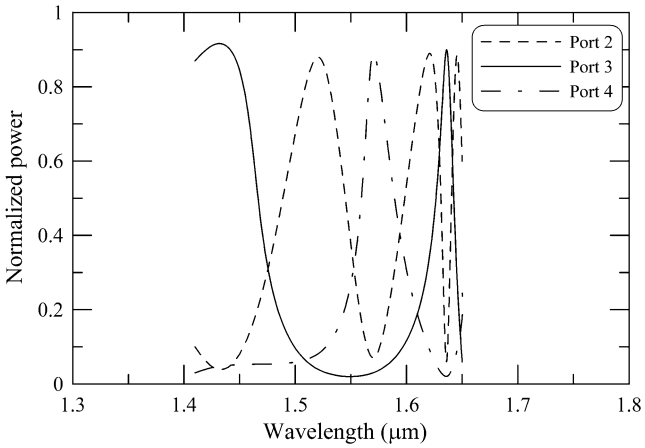

Fig. 15. Transmission spectrum of the square lattice PC WDM splitter with asymmetrical PC couplers.

The WDM splitter based on the triangle lattice PC waveguide couplers is proposed and shown in Fig. 17. Fig. 18 shows the transmission spectrum for the WDM splitter with $L_c = 48a$. This WDM splitter with triangle lattice can work in shorter wavelength regions than the WDM splitter with square lattice, and its wavelength multiplexing properties are numerically investigated. Another WDM splitter with asymmetrical triangle lattice PC waveguide couplers and three output channels is proposed and shown in Fig. 19. Fig. 20 shows the transmission spectrum for this WDM splitter with $L_c = 48a$. The wavelength multiplexing properties of WDM splitter with asymmetrical triangle lattice PC waveguide couplers are similar to those of the WDM splitter with asymmetrical square lattice PC waveguide couplers, and the electric field patterns are also similar. The three-channel multiplexer-demultiplexer in Fig. 10 and Fig. 17 is considered, and the transmission spectrum is shown in Fig. 11 and Fig. 18, respectively. The solid and dashed lines in the transmission spectrum are for the cross and bar states. Assuming the lattice constant a = 0.54 μm, the coupling length for realizing 20 nm channel spacing required in WDM systems is about 144a = 77.76 μm in the structures of Fig. 10 and Fig. 17. The channel spacing of PC couplers is approximately proportional to the coupling length.

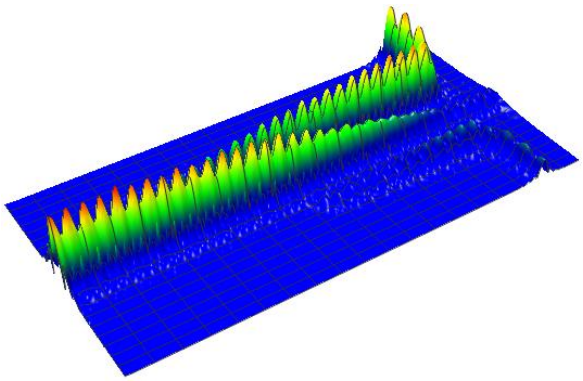

(a) Input wavelength $\lambda_1 = 1.42\ \mu m$

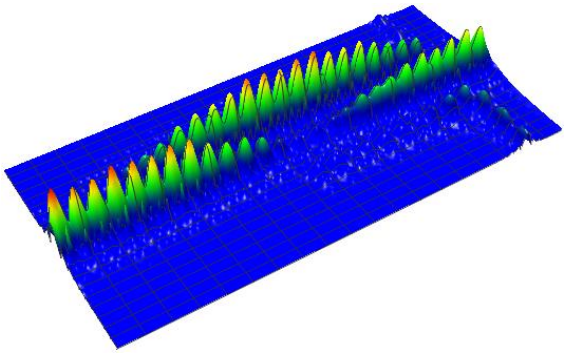

(b) Input wavelength $\lambda_2 = 1.52\ \mu m$

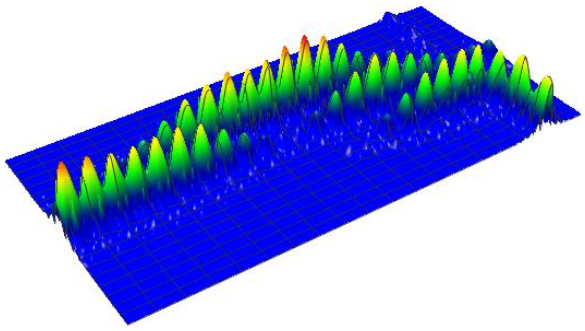

(c) Input wavelength $\lambda_3 = 1.57\ \mu m$

Fig. 16. Electric field patterns of the square lattice PC WDM splitter with asymmetrical PC couplers.

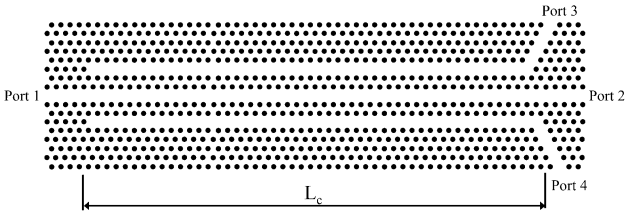

Fig. 17. PC WDM splitter with triangle lattice.

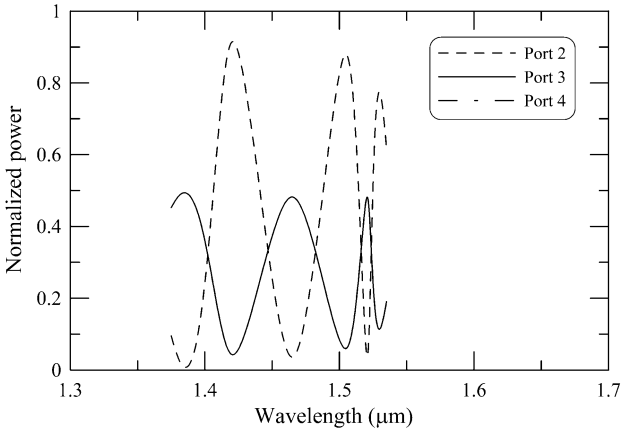

Fig. 18. Transmission spectrum of the triangle lattice PC WDM splitter.

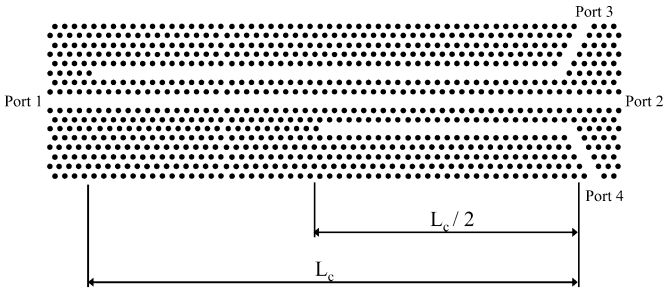

Fig. 19. Triangle lattice PC WDM splitter with asymmetrical PC couplers.

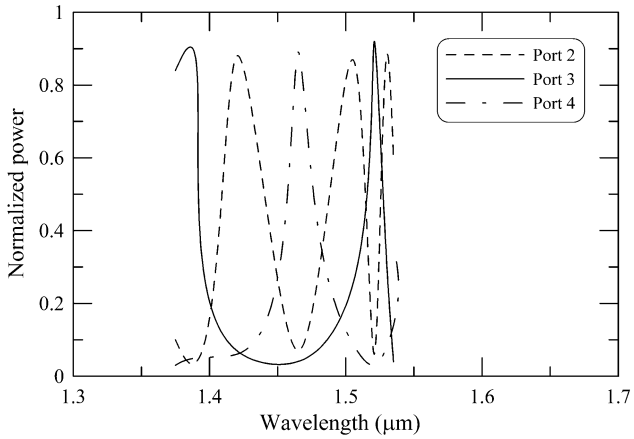

Fig. 20. Transmission spectrum of the triangle lattice PC WDM splitter with asymmetrical PC couplers.

5. Conclusion

In this paper, we have demonstrated numerically a versatile device based on PC technology. The WDM splitters based on square lattice and triangle lattice PC waveguide couplers are proposed and their wavelength multiplexing properties are investigated by using the FDTD method. The coupling lengths of PC waveguide coupler decrease as incident wavelengths increase. At the

same coupling length $L_c = 48a$, the triangle lattice PC waveguide coupler associates with shorter input wavelength than the square lattice PC waveguide coupler. The WDM splitters with symmetrical PC waveguide couplers and three output channels split power equally and transferred it to the opposite guide (port 3, port 4). The WDM splitters with asymmetrical PC waveguide couplers outputted different wavelengths from the different channels, respectively. Compared with traditional WDM device, the sizes of PC WDM splitters are reduced drastically. The WDM splitters can be used as key component to develop micro-scale optical integrated circuits due to their relevant characteristics such as small size, compactness, and mass manufacturing possibilities. The three-dimensional numerical and experimental investigations are needed to take the WDM splitters into realization.

References

[1] E. Yablonovitch, Phys. Rev. Lett. **58**, 2059 (1987).
[2] J. Joannopoulos, R. Meade, J. Winn, Photonic Crystals: Molding the Flow of Light, Princeton University Press, New Jersey (1995).
[3] E. Centeno, D. Felbacq, Opt Commun. **160**, 57 (1999).
[4] B. Little, S. Chu, H. Haus, J. Foresi, J. Laine, J. Lightwave Technol. **17**, 704 (1999).
[5] R. Adar, C. Henry, C. Dragone, R. Kistler, M. Milbrodt, J. Lightwave Technol. **11**, 212 (1993).
[6] H. Kosaka, T. Kawashima, A. Tomita, M. Nomita, T. Tamamura, T. Sato, S. Kawakami, Appl. Phys. Lett. **74**, 1370 (1999).
[7] A. Sharkawy, S. Shi, D. Prather, Appl. Opt. **40**, 2247 (2001).
[8] C. Dragone, J. Lightwave Technol. **7**, 479 (1989).
[9] H. Takahashi, S. Suzuki, I. Nishi, J. Lightwave Technol. **12**, 989 (1994).
[10] K. Hill, Y. Fujii, D. Johnson, B. Kawasaki, Appl. Phys. Lett. **32**, 647 (1978).
[11] E. Centeno, B. Guizal, D. Felbacq, J. Opt. A: Pure Appl. Opt. **1**, L10 (1999).
[12] M. Koshiba, J. Lightwave Technol. **19**, 1970 (2001).
[14] Z. Xu, J. Wang, Q. He, L. Cao, P. Su, G. Jin, Opt. Express **13**, 5608 (2005).
[15] Y. Shi, D. Dai, S. He, IEEE Photonics Technol. Lett. **18**, 2293 (2006).
[16] W. Chiu, T. Huang, Y. Wu, F. Huang, Y. Chan, C. Hou, H. Chien, C. Chen, S. Chen, J. Chyi, J. Lightwave Technol. **26**, 488 (2008).
[17] C.-Y. Liu, Physica E **40**, 2800 (2008).
[18] Y. Shi, S. Anand, S. He, J. Lightwave Technol. **27**, 1443 (2009).
[19] D. Beggs, T. White, L. Cairns, L. O'Faolain, T. Krauss, Physica E **41**, 1111 (2009).
[20] C.-Y. Liu, Phys. Lett. A **373**, 3061 (2009)
[21] C.-Y. Liu, Phys. Lett. A **375**, 2754 (2011).
[22] C.-Y. Liu, J. Mod. Opt. **59**, 218 (2012).
[23] E. Engin, J. O'Brien, M. Cryan, J. Opt. Soc. Am. B **29**, 1157 (2012).
[24] A. Taflove, S. Hagness, Computational Electrodynamics: The Finite Difference Time Domain Method, Artech House, Boston (1998).
[25] M. Koshiba, Y. Tsuji, S. Sasaki, IEEE Microwave Wireless Compon. Lett. **11**, 152 (2001).
[26] H. Benisty, C. Weisbuch, D. Labilloy, M. Rattier, C. Smith, T. Krauss, J. Lightwave Technol. **17**, 2063 (1999).
[27] S. Boscolo, M. Midrio, C. Someda, IEEE J. Quantum Electron. **38**, 47 (2002).

*Corresponding author: cyliu@mail.tku.edu.tw